

000 001 002 003 004 005 006 007 008 009 010 011 012 COCKTAIL-PARTY AT THE MUSEUM: REFERRING AUDIO-VISUAL SEGMENTATION REQUIRES AUGMEN- TATION

013
014
015
016
017
018
019
020
021
022
023
024
025
026
027
028
029
030
031
032
033
034
035
036
037
038
039
040
041
042
043
044
045
046
047
048
049
050
051
052
053
Anonymous authors
Paper under double-blind review

ABSTRACT

Recent advances in Referring Audio-Visual Segmentation (Ref-AVS) have significantly progressed, with the development of multimodal fusion methods and Multimodal Large Language Models (MLLM). However, their modality-specific performance is underexplored, and the effectiveness of audio perception remains unclear. We find that current methods often fail to identify the correct sounding object with audio expressions (e.g., *loudest sounding object*), especially at the cocktail-party (i.e., mixed audio source). In addition, MLLM methods tend to memorize through visual-text patterns due to their weaker audio understanding capabilities. To this end, we first propose **MISA**: Musical-audio Instructed Segmentation Assistant, with an integration of specialized musical-audio encoder MERT, and a musical-specific dataset for alignment to enhance audio tokens' representation. To mitigate the lack of variation of mixed-source signals, we introduce **MUSEUM**, a musical-audio augmentation pipeline consisting of three stages: **M**USical **S**ourc**E**, **A**Ugment, and **M**ix, to respectively perform source separation, sampling from extra musical datasets, and audio augmentation. Our proposed augmentation enriches the mixture of audio signals in the existing training dataset, which facilitates the model learning with diverse samples. Moreover, we refine the existing benchmark as **C-Ref-AVS**bench that categorizes expressions into Audio-Centric (audio cues), AV-Grounded (audio and visual cues), and Visual-Centric (visual cues), in order to perform modality-specific evaluation. Our approach achieves state-of-the-art performance on both Ref-AVSbench and C-Ref-AVSbench, particularly with the Audio-Centric expressions.

1 INTRODUCTION

Audio and visual information are essential in our daily lives. One of humans' abilities is to locate and focus on an interesting-sounding source within a cocktail-party scene (i.e., mixed audio source), e.g., the one talking in a foreign language. In a musical environment, most duet performers perform in dense and overlapping sound (You et al., 2025), and thus humans' selective attention can help distinguish the sound source by different sound characteristics, e.g., "loudest sound instrument". This phenomenon creates an opportunity to model the ability into machine intelligence, enabling machines to understand the environment through sight and sound.

A relevant topic is Referring Audio-Visual Segmentation (Ref-AVS) (Wang et al., 2024b), which aims to segment the target object in an audio-visual scene, given natural language expressions. The expressions involve multiple scenarios, including Audio-Centric (audio cues), AV-Grounded (audio & visual cues), and Visual-Centric (visual cues), allowing model to decide which modality should be leveraged and fused (examples provided in Fig. 1). While the pioneering works (Wang et al., 2024b; 2025a; Radman & Laaksonen, 2025; Liu et al., 2025) focus on developing multimodal transformer fusion modules with a segmentation model (Cheng et al., 2022; Kirillov et al., 2023; Ravi et al., 2024), recent works leverage Multimodal Large Language Model (MLLM) for improvement (Du et al., 2025; Ying et al., 2025; Zhou et al., 2025; Zhong et al., 2025; Luo et al., 2025). Although these methods have made significant progress, the performance across each modality-specific scenario needs to be further studied, and the effectiveness of the audio signal remains unclear.

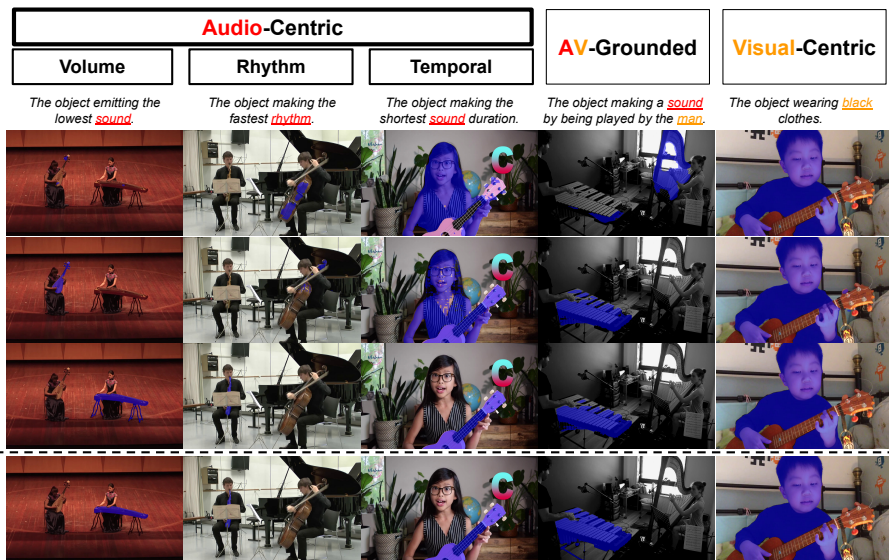


Figure 1: **Samples and performance on each scenario.** Expressions either occur **audio** cues or **visual** cues, or both involve **(audio & visual)**. While most methods can perform well in **Visual-Centric** scenarios, EEMC (Wang et al., 2024b) and finetuned Sa2VA-1B (Yuan et al., 2025) fail to segment the sounding object with **Audio-Centric** expressions. In addition, even finetuned Sa2VA-1B only uses visual-text input, it is able to segment sounding object within the **AV-Grounded** scenario, suggesting the need to evaluate the audio perception capabilities through modality-specific scenarios (e.g., use **Audio-Centric** subset for performance assessment). Our method, **MISA + MUSEUM**, which integrates audio modality into MLLM-based segmentation model with the augmentation strategy to enrich the diversity of audio training samples, achieves better performance of segmenting the sounding objects across all scenarios.

For instance, the first row of Fig. 1 shows the performance by each scenario using the state-of-the-art (SOTA) method, EEMC (Wang et al., 2024b). This method fails to segment the sounding object, indicating that the audio perception is weaker. In addition, we finetune the SOTA of MLLM-based segmentation model, Sa2VA-1B (Yuan et al., 2025), for such tasks without audio guidance. We find that, even such model does not take the audio modality into its computation (i.e., using visual-text input only), with solely leveraging the text in the expression and the input image, the substantial improvement can already be made (see the fourth column in Fig. 1 in AV-Grounded, compared to EEMC). While this model brings a strong baseline, it performs worse in Audio-Centric scenarios within a cocktail-party scene, where the audio signal is needed to disambiguate various expressions.

Based on the observations of the aforementioned methods (i.e., EEMC and Sa2VA-1B), we propose **MISA**: **M**usical-**A**udio **I**nstructed **S**egmentation **A**ssistant, which integrates and aligns audio modality into a MLLM-based segmentation model. It adopts Sa2VA-1B (Yuan et al., 2025), followed by integrating a musical-audio encoder MERT (Li et al., 2023b) and using musical-audio datasets (Kim et al., 2019; Liu et al., 2023b) for alignment, to build a musical-audio-aware MLLM-based segmentation model. While this helps encode audio representation, substantial variation of audio signals is crucial to eliminate the potential modality bias (i.e., the model would prefer to utilize the visual or text information). Hence, we introduce **MUSEUM**, a musical-audio augmentation pipeline consisting of **M**USical **S**ourc**E**, **A**Ugment, and **M**ix stages. Specifically, given a video composed of multiple sounding objects with their ground truth segmentation masks, we perform augmentations upon the audio sources of these objects and their corresponding keywords/expressions. For example, given a video with playing violin and cello, and its expression keyword “loudest”, we increase the volume of the violin’s audio source while decreasing the cello’s to become weaker than the violin’s, in which the resultant augmented sample has the corresponding ground truth segmentation mask upon the violin and the expression of “The loudest sounding object.”

As a result, our strategies produce training samples (each is composed of an input video, the expression, and the ground truth segmentation mask) with considerable variation of audio signals, which facilitates the model learning to be aware of Audio-Centric scenarios (see Fig. 2). Moreover, evaluating modality-specific scenarios’ performance (i.e., Audio-Centric, AV-Grounded, Visual-Centric)

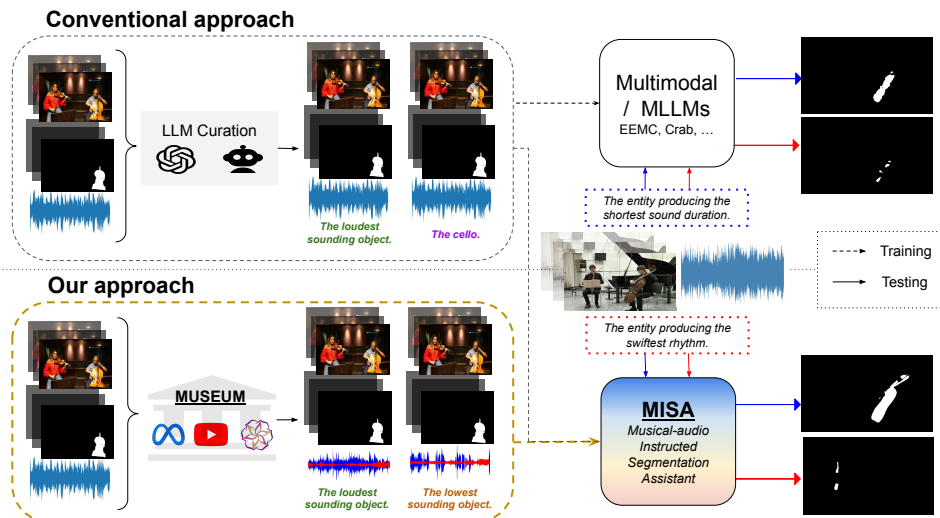


Figure 2: **Comparisons with conventional approaches.** Conventional approach curates the dataset by human labeler or LLMs, generating various natural language expressions for a sample of video with audio and its ground truth segmentation mask (for the sounding object targeted by the expression). While it helps to create numerous samples with different expressions, as the audio signal is fixed within the video, the model would lean towards learning to leverage more with text and visual modalities which typically have more variation than the audio one, thus leading to weaker audio signal learning. We propose **MUSEUM** to augment audio signals, generate substantial variation of mixture audio sources to guide the learning process of our model, **MISA**, to be aware of the differences of audio signals. Our approach hence better segments the sounding object with Audio-Centric expressions (e.g., our model successfully segments the “saxophone” with expression: “**The entity producing the swiftest rhythm.**”).

is crucial to understand model’s capabilities that leverage model-specific information from the input video and its textual content in the expression. While the original Ref-AVSbench testing set lacks modality-specific information about the expression, we improve the benchmark, denoted as **C-Ref-AVSbench**, by labeling modality-specific information on expressions (e.g., given an expression, “The loudest sounding object”, it is labeled as Audio-Centric since the “sounding” keyword exists).

In summary, our main contributions are as follows: (1) We propose **MISA**, a MLLM-based segmentation model that empowers with musical-audio awareness capabilities; (2) We introduce **MUSEUM**, a musical-audio augmentation pipeline to enrich the audio signals and facilitate the audio differentiating capabilities; (3) We refine the benchmark as **C-Ref-AVSbench** to evaluate modality-specific scenarios; (4) Our method achieves SOTA performance on Ref-AVSbench and C-Ref-AVSbench, improves significantly with Audio-Centric expressions (see Fig. 1). We will release the dataset, code, and models to the public for reproducibility.

2 RELATED WORKS

Referring Audio-Visual Segmentation. Ref-AVS is the intersection of Referring Video Object Segmentation (RVOS) (Ding et al., 2025) and Audio Visual Segmentation (AVS) (Zhou et al., 2023; 2022), where it aims to produce a binary mask by the guidance of text and audio. EEMC (Wang et al., 2024b) is first proposed by implementing a multimodal transformer for audio-visual-text fusion, followed by Mask2Former (Cheng et al., 2022) to produce segmentation results. Building upon this, several works (Wang et al., 2025a; Radman & Laaksonen, 2025; Liu et al., 2025) enhance the segmentation capabilities by integrating SAM (Kirillov et al., 2023) and SAM 2 (Ravi et al., 2024). Recent studies have utilized Multimodal Large Language Model (MLLM) with a segmentation model (Lai et al., 2024; Yan et al., 2024; Yuan et al., 2025). Crab (Du et al., 2025) unifies multitask audio-visual understanding and segmentation within a MLLM (Chen et al., 2023), while OISA (Ying et al., 2025) proposes a MLLM segmentation model upon omnimodal expressions. Omni-R1 (Zhong et al., 2025), TGS-Agent (Zhou et al., 2025), and AURORA (Luo et al., 2025) further propose to train MLLM as a reasoning model by utilizing Chain of Thought (Wei et al., 2022).

162 Despite their stronger visual-text understanding, the limited mixture of audio sources and weaker
 163 audio representation hinder the performance in the Audio-Centric scenarios. Hence, we introduce
 164 a learning framework for enhancing the musical-audio awareness and achieving better audio-based
 165 disambiguation ability, with the help of our proposed augmentation strategy to enrich data variation.

166 **Multimodal Large Language Models.** MLLM is predominant in multimodal learning. While most
 167 existing MLLMS are basically Vision Language Models (Liu et al., 2023a; Chen et al., 2024) (i.e.
 168 only taking visual and textual modalities as input), they can be used as the bases for learning to
 169 include the additional audio modality (Cheng et al., 2024; Xu et al., 2025; Chowdhury et al., 2025).
 170 For processing the input audio signals into tokens, audio encoders such as BEATs (Chen et al.,
 171 2023), Whisper (Radford et al., 2023), MERT (Li et al., 2023b) are utilized respectively for general
 172 audio, speech, and music, while they usually require large-scale audio-text dataset for pretraining
 173 and alignment (Kim et al., 2019; Chen et al., 2021). In our proposed framework, we also adopt
 174 MLLM as our base model and attempt to integrate the additional audio modality. As our scenario
 175 is mainly on musical cocktail-party scenes, we leverage musical-specific components (e.g. MERT)
 176 into our model to have a better musical-audio awareness.

177 **Audio Augmentation and Mixing.** Data augmentation is a common and effective technique to help
 178 model training and improve its generalizability, which requires manipulating the existing dataset to
 179 enrich the diversity of training samples (Wang et al., 2025b). Several audio augmentation methods,
 180 e.g., loudness modification and time stretch (Uhlich et al., 2017; Prétet et al., 2019) have been
 181 studied for automatic speech recognition (Park et al., 2019; Ko et al., 2015). Recently, remixing
 182 approaches which attempt to mix-up two audio signals also become popular for speech and sound-
 183 related tasks (Kim et al., 2021; Meng et al., 2021) or audio/music source separation (Jeon et al., 2024;
 184 Rouard et al., 2022; Défossez et al., 2021). Inspired by them, we propose an audio augmentation
 185 pipeline to enrich audio signal diversity. However, distinct from these approaches that primarily
 186 aim for signal invariance, our pipeline focuses on enhancing audio differentiating capabilities by
 187 simulating diverse mixture sources within the same visual context. This strategy is specifically
 188 designed to mitigate the modality bias (i.e., the model would prefer to utilize the visual or text
 189 information) prevalent in the Ref-AVS task.

190 3 PROPOSED METHOD

192 3.1 MISA: MUSICAL-AUDIO INSTRUCTED SEGMENTATION ASSISTANT

194 We introduce **MISA**, a Musical-audio Instructed Segmentation Assistant, with the highlights of
 195 the usage of audio encoder MERT, alignment using multiple datasets, and a training strategy with
 196 rejection supervision, to form a model having the better musical-audio awareness. Fig. 3 illustrates
 197 the training procedure of our proposed MISA model.

199 **Model Architecture.** We start from a MLLM-based segmentation framework, which includes a
 200 MLLM for multimodal understanding and a segmentation model for mask generation. We adopt
 201 Sa2VA-1B (Yuan et al., 2025) as our visual-language backbone, which consists of 1) a Visual En-
 202 coder with InternViT-300M-448px (Chen et al., 2024), followed by a two-layer MLP Vision Projec-
 203 tor, 2) a LLM backbone with Qwen2.5-0.5B-Instruct (Qwen et al., 2025), a two-layer MLP Prompt
 204 Projector for projecting the $[SEG]$ token, which is a special token for segmentation prompting, and
 205 3) a SAM 2 model (Ravi et al., 2024) as a segmentation mask generation module. Next, we integrate
 206 the audio branch into the model by leveraging MERT (Li et al., 2023b) as the MLLM audio branch’s
 207 encoder (i.e. a specialized audio encoder pretrained on a musical-audio dataset and musical-acoustic
 208 objective), followed by a two-layer MLP Audio Projector, to learn and capture the dense acoustic
 209 representation.

210 Given video frames with audio input and expression, the visual branch first processes K frames indi-
 211 vidually, obtaining vision tokens as denoted as $V = \{v_1, v_2, \dots, v_K\}$, where $v_k \in \mathbb{R}^{L_v \times d}$ represents
 212 L_v vision tokens in k -th frame with d dimensions; the audio branch processes audio clip, obtaining
 213 audio tokens as denoted as a , where $a \in \mathbb{R}^{L_a \times d}$ represents L_a audio tokens with d dimensions; ex-
 214 pressions are embedded as x , where $x \in \mathbb{R}^{L_x \times d}$ represents L_x text tokens with d dimensions. Next,
 215 we organize vision, audio, and text tokens into $X = \{x_v, v_1, v_2, \dots, v_N, x_v, a, x_a, x\}$ to form a
 216 sequence input for MLLM, where $x_v, x_a \in \mathbb{R}^{1 \times d}$ represent special tokens for the vision tokens and
 217 audio tokens. This MLLM will be trained to generate $[SEG]$ token x_s , where $x_s \in \mathbb{R}^{1 \times d}$, and use

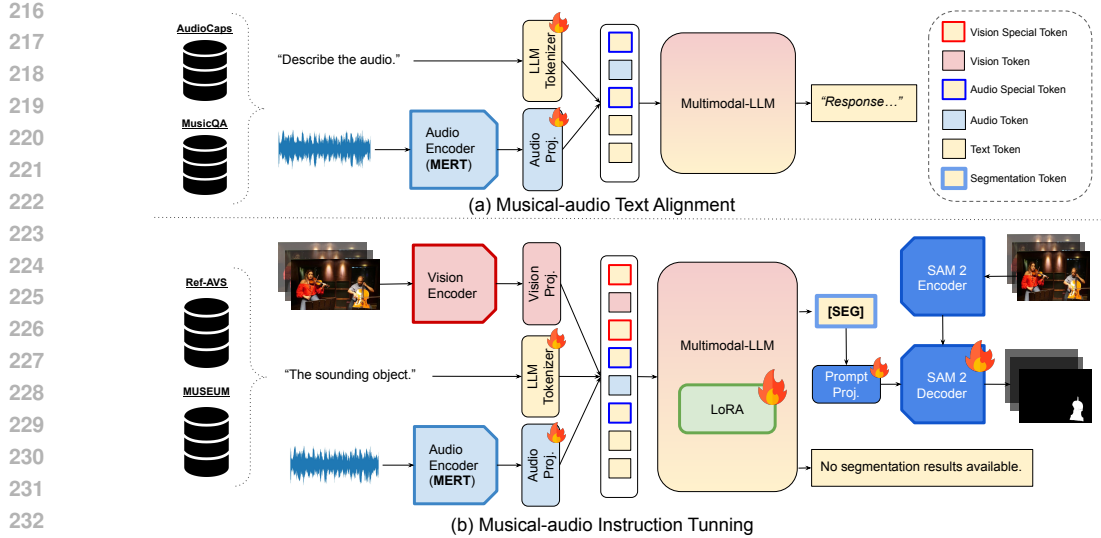


Figure 3: **MISA.** (a) Musical-audio Text Alignment: We train the Audio Projector and Text Tokenizer in this stage, while other parameters are frozen. (b) Musical-audio Instruction Tuning: We finetune the Audio Projector, Text Tokenizer, Prompt Projector, SAM 2 Decoder, while other parameters are frozen. In addition, Multimodal-LLM is fine-tuned via LoRA (Hu et al., 2021).

as a prompt to guide the segmentation module in producing mask $M = \{m_1, m_2, \dots, m_K\}$, where $m_k \in \mathbb{R}^{Height \times Width}$.

Training Paradigm and Objectives. Our training paradigm includes a musical-audio text alignment stage and a musical-audio instruction tuning stage. Injecting a new modality into MLLM requires pretraining with a modality-specific dataset, so we use AudioCaps (Kim et al., 2019) and MusicQA (Liu et al., 2023b) to build the general and domain-specific representation alignment. During this stage, we employ an autoregressive cross-entropy loss, L_{txt} , to train the model on audio captioning tasks. The objective of L_{txt} is to align the acoustic representations from the audio encoder MERT with the MLLM’s text embedding space. By training the model to “describe the audio,” we ensure that the audio tokens are semantically meaningful to the MLLM prior to fine-tuning for segmentation.

Next, we perform musical-audio instruction tuning for the Ref-AVS task. We optimize the model by the combination of autoregressive cross-entropy loss L_{txt} and segmentation loss L_{seg} composed with binary cross-entropy loss and dice loss. In practice, the object described by an expression may be unavailable (e.g., the query targets a “sounding object,” but no object is sounding within the visual scene). Unlike prior works, which typically enforce the segmentation model to produce a zero mask given unavailable references, we choose to bypass segmentation in these cases to avoid hindering the model’s ability to distinguish valid signals. Instead, the model is trained to output a text-based rejection response (i.e., “No segmentation results available.”) if the reference is unavailable. This Rejection Supervision training objective is modified as follows:

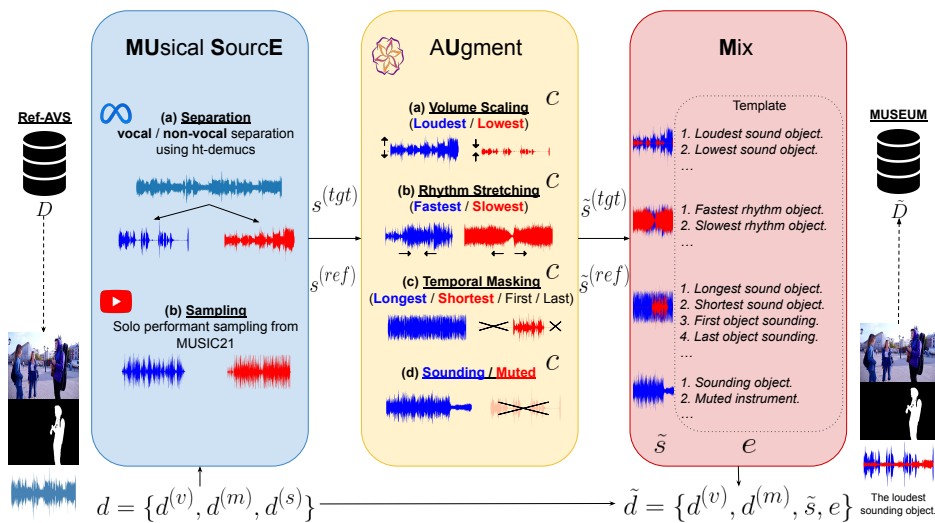
$$L_{instruction} = \begin{cases} L_{txt} + L_{seg}, & \text{if } M \notin \emptyset, \\ L_{txt}, & \text{otherwise.} \end{cases} \quad (1)$$

3.2 MUSEUM: MUSICAL-AUDIO AUGMENTATION

This section introduces **MUSEUM**, a musical-audio augmentation pipeline which consists of **MU**sical **Sou**rcE, **A**ugment, and **M**ix stages. The objective is to augment multiple audio signals within the dataset D , creating various audio-differentiate samples given visual frames, ground truth segmentation mask, audio signal, and expression keyword c (e.g., “loudest”, used to decide the augmentation method), which generate variation of cocktail-party scenes. These augmented samples form an additional dataset \tilde{D} for model training. Fig. 4 demonstrates the overall pipeline.

MUtical **Sou**rcE. We first obtain the audio signals by the guidance of the video and its ground truth segmentation masks. Given a video sample with multiple objects/masks, and $d =$

270
271
272
273
274
275
276
277
278
279
280
281
282
283
284
285
286



287
288
289
290
291
292
293
294
295
296
297
Figure 4: **MUSEUM**. Given the Ref-AVS dataset D , we augment the samples to form an augmented dataset \tilde{D} . We sample $d = \{d^{(v)}, d^{(m)}, d^{(s)}\} \in D$, corresponding to the sample of visual frames, ground truth segmentation masks, and audio signal. We first extract target $s^{(tgt)}$ and reference $s^{(ref)}$ signals by one of the operations (i.e., Separation or Sampling) given d , in which we can obtain the scene information to decide the operation. Next, we augment the two signals to $\tilde{s}^{(tgt)}$ and $\tilde{s}^{(ref)}$ by using one of the augmentations (i.e., Volume Scaling, Rhythm Stretching, Temporal Masking, Sounding/Muted) given random sampled expression keyword c (e.g., “loudest”); Finally, we mix two signals into \tilde{s} and sample an expression e (e.g., “The loudest sounding object.”) given predefined expressions template and c . Then these outputs form a final augmented sample $\tilde{d} = \{d^{(v)}, d^{(m)}, \tilde{s}, e\}$, corresponding to the augmented sample of visual frames, ground truth segmentation masks, augmented mixture audio, and corresponding expressions.

298
299
300
301
302
 $\{d^{(v)}, d^{(m)}, d^{(s)}\} \in D$ denoted as the sample of visual frames, ground truth segmentation masks, and audio signal, we random sample an expression keyword c , assign the ground truth segmentation masks’ category as target object $c^{(tgt)}$ and another category within video as reference object $c^{(ref)}$. We choose one of the operations to obtain the target and reference signal, denoted as $s^{(tgt)}$ and $s^{(ref)}$:

303
304
305
306
307
308
(a) Separation: In the vocal and non-vocal scenes, we augment the existing audio source by separating it into vocal and non-vocal signals, denoted as $s^{(voc)}$ and $s^{(nov)}$, by leverage ht-demucs (Rouard et al., 2022) denoted as f_{sep} , which is a hybrid spectrogram transformer model for music source separation, with advantages in the separation of vocal and non-vocal. We then assign signals according to $c^{(tgt)}$ and $c^{(ref)}$ as follows:

$$s^{(voc)}, s^{(nov)} = f_{sep}(d^{(s)}), \quad (2)$$

$$s^{(tgt)}, s^{(ref)} = \begin{cases} s^{(voc)}, s^{(nov)}, & \text{if } c^{(tgt)} \text{ corresponds to } s^{(voc)}, \\ s^{(nov)}, s^{(voc)}, & \text{if } c^{(tgt)} \text{ corresponds to } s^{(nov)}. \end{cases} \quad (3)$$

309
310
311
312
313
(b) Sampling: While separating mixture audio source of multiple instruments is non-trivial, we sample audio signals from an extra dataset, MUSIC21 (Zhao et al., 2019) denoted as D_M , which is an audio-visual source separation dataset consisting various solo performant videos, given the category condition $c^{(tgt)}, c^{(ref)}$, to enhance the audio variation.

$$s^{(tgt)} \sim D_M | c^{(tgt)}, s^{(ref)} \sim D_M | c^{(ref)}. \quad (4)$$

314
315
316
317
318
AUGment. In this stage, we perform audio augmentation for the individual signals from the previous stage. The objective is to simulate a variant of acoustic properties given a sampled expression keyword c , within complex cocktail-party scenes. The augmentation methodologies include Volume Scaling, Rhythm Stretching, Temporal Masking, and Sounding/Muted. These methods are combined to form the augmentation function F_{aug} . The augmented target and reference signal are computed as:

324
325
326

$$\tilde{s}^{(tgt)}, \tilde{s}^{(ref)} = F_{aug}(s^{(tgt)}, s^{(ref)}, c). \quad (5)$$

327 (a) **Volume Scaling:** Adjusting the amplitude of an audio signal to simulate variations in loud-
328 ness. Given an audio signal $s(t)$, volume scaling applies a multiplicative factor $\alpha \in \mathbb{R}^+$:
329 $\tilde{s}(t) = \alpha \cdot s(t)$.

330 (b) **Rhythm Stretching:** Modifying the rhythm of an audio signal by using short-time Fourier
331 transform (STFT), phase vocoder, and inverse STFT, which are implemented with lib-
332 brosa (McFee et al., 2025), to manipulate the signal along the time axis in the time-
333 frequency domain. This is achieved by scaling audio duration by a stretch factor $\gamma \in \mathbb{R}^+$:
334 $\tilde{s}(t) = s(\gamma \cdot t)$.

335 (c) **Temporal Masking:** Masking portions of the audio signal along the time axis, specified
336 by a time region in $\mathcal{T} = [t_0, t_0 + \Delta t]$, where $t_0 \sim U(0, T - \Delta t)$ refers to a randomly
337 chosen start index; Δt refers to mask length (duration); T refers to length of audio signal:
338 $\tilde{s}(t) = \mathbf{1}[t \notin \mathcal{T}] \cdot s(t)$.

339 (d) **Sounding/Muted:** A special case of Temporal Masking, where we simulate single sound
340 source within multiple audible objects in the scene. If $\mathcal{T} = \emptyset$, the entire signal is preserved
341 as $\tilde{s}(t) = s(t)$; If $\mathcal{T} = [0, T]$, the entire signal is dropped as $\tilde{s}(t) = 0$.

342 **Mix.** Lastly, we add the augmented target and reference signals to form a new mixture audio sig-
343 nal \tilde{s} . We then sample an expression e from predefined expression template given the expression
344 keyword c , producing a new augmented sample $\tilde{d} = \{d^{(v)}, d^{(m)}, \tilde{s}, e\}$, $\tilde{d} \in \tilde{D}$, corresponding to the
345 augmented sample of visual frames, ground truth segmentation masks, augmented mixture audio,
346 and expression.

347 4 C-REF-AVS BENCH

348 We propose **C-Ref-AVS BENCH**, refined from the Ref-AVS BENCH (Wang et al., 2024b) Seen subset.
349 Originally, Ref-AVS BENCH lacks interpretation of the modality-specific performance. To delve into
350 the performance understanding, we separate the expressions into three types: Audio-Centric, AV-
351 Grounded, and Visual-Centric. Audio-Centric and AV-Grounded are related to audio cues, while
352 Visual-Centric is unrelated to audio cues. We label it using keyword extraction. When the expres-
353 sions include keywords such as “sound” and “audio”, we refer to this as audio cues; otherwise,
354 we assign them as Visual-Centric. Next, we categorize the samples with audio cues by identify-
355 ing whether expressions include explicit, spatial, or semantic queries (e.g., “singing”, “left to”, or
356 “piano”). We assign these expressions to AV-Grounded; otherwise, assign as Audio-Centric.

357 These labels help assess the model’s modality-specific capabilities, evaluate audio-awareness by
358 not being biased by the explicit text (e.g., “The loudest sounding object” will be labeled as Audio-
359 Centric to help assess audio-awareness, while “The sounding object louder than piano” will be
360 labeled as AV-Grounded to avoid the biased information from the semantic keyword “piano”). In
361 addition, we add extra subcategories for Audio-Centric: Volume, Temporal, and Rhythm, with the
362 keywords such as “loudest”, “fastest”, “longest”, guiding us in evaluating specific scenarios.

363 Furthermore, we find that several videos occur in both the training and testing sets. Although they
364 are sampled from different timestamps, it might misinterpret the modality-specific performance, as
365 it merely memorizes visual scenes with a fixed expression. We remove these videos that exist within
366 the training and testing sets by identifying the shared video ID given by the dataset. We provide the
367 examples of the removed video and statistics of C-Ref-AVS BENCH in Appendix A.2.

370 5 EXPERIMENTAL RESULTS

371 5.1 EXPERIMENTAL SETTINGS

372 **Datasets.** We evaluate our methods on the Ref-AVS BENCH (Wang et al., 2024b). It consists of a
373 training set (2,908 videos), a validation set (276 videos), and a testing set (818 videos). The testing
374 set is divided into three subsets: *Seen* (292 videos) with trained categories, *Unseen* (269 videos)
375 with 13 novel categories, and *Null*, which refers to nothing to segment. For the details and ablation
376 studies, we evaluate through **C-Ref-AVS BENCH**.

378 Table 1: **Results on Ref-AVSbench.** Mix is the average of Seen and Unseen. * denotes different
 379 implementations from the original Segmentation Arch.; \dagger denotes the usage of frozen SAM 2 as a
 380 standalone agent. Gray row is the visual-text SOTA. Blue row is our best model.

Method	MLLM Arch.	Seg. Arch.	Seen			Unseen			Mix (S+U)			Null S
			\mathcal{J}	\mathcal{F}	$\mathcal{J} \& \mathcal{F}$	\mathcal{J}	\mathcal{F}	$\mathcal{J} \& \mathcal{F}$	\mathcal{J}	\mathcal{F}	$\mathcal{J} \& \mathcal{F}$	
<i>Audio-based methods</i>												
AVSBench (Zhou et al., 2022)	-	-	23.2	51.1	37.2	32.4	54.7	43.5	27.8	52.9	40.3	20.8
AVSegFormer (Gao et al., 2024)	-	-	33.5	47.0	40.2	36.1	50.1	43.1	34.8	48.6	41.7	17.1
GAVS (Wang et al., 2024a)	-	-	28.9	49.8	39.4	29.8	49.7	39.8	29.4	49.8	39.6	19.0
<i>Visual-based methods</i>												
ReferFormer (Wu et al., 2022)	-	-	31.3	50.1	40.7	30.4	48.8	39.6	30.9	49.5	40.2	17.6
R2VOS (Li et al., 2023a)	-	-	25.0	41.0	33.0	27.9	49.8	38.9	26.5	45.4	35.9	18.3
<i>Multimodal-based methods</i>												
EEMC (Wang et al., 2024b)	-	M2F	34.2	51.3	42.8	49.5	64.8	57.0	41.9	58.1	50.0	0.7
SAM2-LOVE (Wang et al., 2025a)	-	SAM 2	43.5	51.9	47.7	66.5	72.3	69.4	55.0	62.1	58.5	23.0
TSAM (Radman & Laaksonen, 2025)	-	SAM-B	43.4	56.8	50.1	54.6	66.4	60.5	49.0	61.6	55.3	1.7
AuralSAM2 (Liu et al., 2025)	-	SAM 2	56.2	61.2	58.7	68.7	74.4	71.5	62.4	67.8	65.1	6.5
<i>MLLM-based methods</i>												
Crab (Du et al., 2025)	LLaMA2-7B-Chat	SAM*	40.5	58.0	49.3	45.6	63.0	54.3	43.1	60.5	46.2	-
OISA-1B (Ying et al., 2025)	InternVL2.5-1B	M2F*	51.7	58.7	55.2	58.3	65.1	61.7	54.5	61.4	58.0	9.8
Omni-R1 (Zhong et al., 2025)	Qwen2.5-Omni-7B	SAM 2 \dagger	43.0	51.4	47.2	63.1	69.3	66.2	53.1	60.4	56.7	-
TGS-Agent (Zhou et al., 2025)	LLaMA2-7B-Chat	SAM 2 \dagger	49.5	60.4	54.9	73.2	80.6	76.9	61.3	70.5	65.9	3.5
AURORA (Luo et al., 2025)	VideoLLaMA2-7B	SAM	63.2	72.8	68.0	69.7	76.4	73.0	66.5	74.6	70.1	-
Sa2VA-1B (Yuan et al., 2025)	InternVL2.5-1B	SAM 2	41.8	56.6	49.2	63.6	76.8	70.2	52.7	66.7	59.7	-
Sa2VA-1B (<i>finetuned</i>)	InternVL2.5-1B	SAM 2	75.3	85.4	80.3	81.1	87.9	84.5	78.2	86.6	82.4	7.9
<i>Ours</i>												
MISA	InternVL2.5-1B	SAM 2	76.4	86.5	81.4	80.7	88.4	84.6	78.6	87.5	83.0	7.0
MISA + MUSEUM	InternVL2.5-1B	SAM 2	77.0	87.0	82.0	81.3	88.2	84.7	79.1	87.6	83.4	1.3

398 Table 2: **Results on C-Ref-AVSbench.** Gray row is the visual-text SOTA.

Method	Audio-Centric			AV-Grounded			Visual-Centric			Overall		
	\mathcal{J}	\mathcal{F}	$\mathcal{J} \& \mathcal{F}$	\mathcal{J}	\mathcal{F}	$\mathcal{J} \& \mathcal{F}$	\mathcal{J}	\mathcal{F}	$\mathcal{J} \& \mathcal{F}$	\mathcal{J}	\mathcal{F}	$\mathcal{J} \& \mathcal{F}$
<i>SOTA methods</i>												
EEMC (Wang et al., 2024b)	45.7	67.2	56.5	43.1	63.1	53.1	35.7	54.7	45.2	42.5	62.9	52.7
Crab (Du et al., 2025)	39.9	61.3	50.6	22.5	43.4	32.9	21.5	40.7	31.1	28.0	48.7	38.4
Sa2VA-1B (Yuan et al., 2025)	36.0	55.8	45.9	44.8	60.7	52.7	63.9	75.6	69.8	45.5	61.9	53.7
Sa2VA-1B (<i>finetuned</i>)	70.9	84.2	77.6	79.3	88.4	83.9	79.8	88.3	84.0	76.6	87.0	81.8
<i>Ours</i>												
MISA	76.2	87.2	81.7	79.3	89.3	84.3	78.2	87.5	82.9	78.1	88.3	83.2
MISA + MUSEUM	81.6	91.2	86.4	79.3	89.3	84.3	78.6	88.1	83.4	79.9	89.7	84.8

407 **Evaluation Metrics.** Following the evaluation protocol from (Wang et al., 2024b; Zhou et al., 2022),
 408 we adopt the Jaccard Index (\mathcal{J}), the F-score (\mathcal{F}), and their average ($\mathcal{J} \& \mathcal{F}$) as primary evaluation
 409 metrics. A metric S is employed for the Null set, which is the ratio between predicted mask area
 410 and the background area; lower is better in this case.

411 **Implementation Details.** We first perform musical-audio text alignment for two epochs using a
 412 1e-4 learning rate and a batch size of 4 per GPU. Next, we finetune with Ref-AVS and **MUSEUM**
 413 for three epochs with a learning rate of 4e-4 and a batch size of 1. LoRA (Hu et al., 2021) rank is set
 414 to 128 and a scaling factor of 256. AdamW optimizer and bfloat16 precision are applied for model
 415 training. All experiments are conducted on 8 NVIDIA RTX A5000 GPUs.

417 5.2 MAIN RESULTS

419 In the following, we evaluate our methods by comparing it with previous SOTA methods. We
 420 present our methodologies as MISA and MISA + MUSEUM, representing the usage without and
 421 with MUSEUM. In addition to the existing SOTA, we add visual-text models as references: Sa2VA-
 422 1B (Yuan et al., 2025), and a finetuned version denoted as Sa2VA-1B (*finetuned*).

423 **Ref-AVSbench.** Table 1 shows the overall results on Ref-AVSbench. Our **MISA** achieves better
 424 performance than SOTAs in terms of a similar or smaller MLLM backbone and segmentation ar-
 425 chitecture (e.g., comparing to a larger MLLM backbone AURORA (Luo et al., 2025), our model
 426 achieves better results.). Moreover, using **MUSEUM** with MISA further improves the overall per-
 427 formance. Our methods also gain improvements against Sa2VA-1B (Yuan et al., 2025), which is the
 428 highest result of the existing SOTA. Nevertheless, the remarkably high performance of the visual-
 429 text SOTA implies that the original benchmark allows for visual-text shortcut learning without lever-
 430 aging audio modality. This observation necessitates our refined **C-Ref-AVSbench** evaluation (Ta-
 431 ble 2), which explicitly isolates modality-specific scenarios, especially the Audio-Centric scenario,
 432 to assess true cross-modal reasoning capabilities.

432 **Table 3: Ablation study of augmentation within MU-
433 SEUM.** Results are reported using \mathcal{J} & \mathcal{F} .

Augmentation	V.	T.	R.	S.	M.	Audio-Centric	Overall	V.	T.	R.
						81.7	83.2	73.7	79.1	68.8
✓						81.7	83.4	79.3	76.8	72.1
	✓					84.5	83.8	78.2	84.9	86.1
		✓				82.4	83.3	72.3	78.8	70.8
			✓			84.5	83.8	78.9	84.6	74.1
<i>Ours</i>		✓	✓	✓	✓	86.4	84.8	83.9	83.9	90.2

441 **Table 5: Ablation study of rejection supervision.**

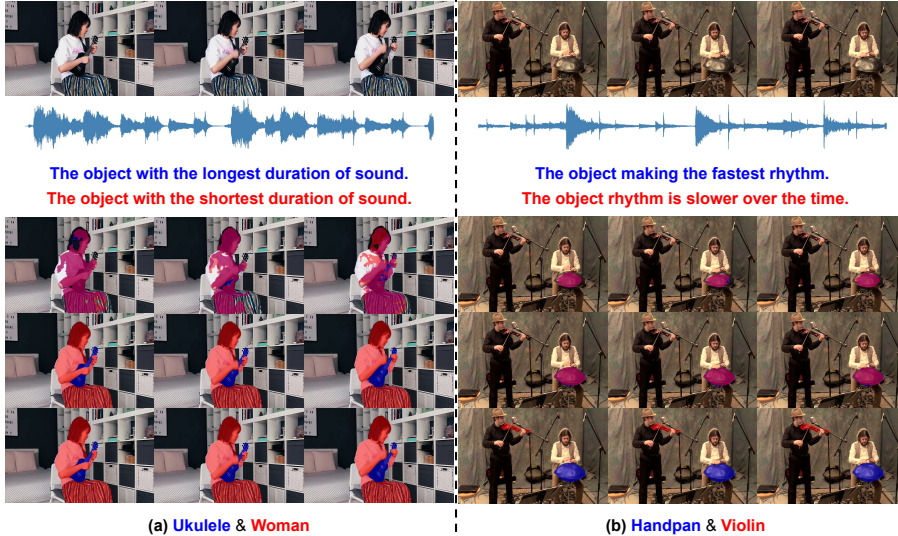
Rejection Supervision	C-Ref-AVSbench	Ref-AVSbench	Audio-Centric	Overall	\mathcal{J} & \mathcal{F}	Null	\mathcal{S}
Without	82.3	83.8		1.3			
With (Ours)		86.4	84.8	1.3			

442 **Table 4: Ablation study of audio en-
443 coder with \mathcal{J} & \mathcal{F} .**

Audio Encoder	Audio-Centric	Overall
BEATs	83.2	83.1
Whisper	81.6	83.0
<i>Ours</i>		
MERT	86.4	84.8

444 **Table 6: Ablation study of alignment**
445 **datasets with \mathcal{J} & \mathcal{F} .**

AudioCaps	MusicQA	Audio-Centric	Overall
✓		77.8	80.9
	✓	83.6	82.1
		82.8	81.6
<i>Ours</i>	✓	86.4	84.8



446 **Figure 5: Qualitative results across different expressions within audio-visual pairs.** Both exam-
447 ples show the results with Audio-Centric expression from EEMC, MISA, and MISA + MUSEUM.
448 We combine the segmentation results of different expressions and our method produces the high
449 quality and precision segmentation compared to EEMC.

450 **C-Ref-AVSbench.** Table 2 shows the results on C-Ref-AVSbench across different expression
451 groups. While the Sa2VA-1B (Yuan et al., 2025) has a strong performance in the Visual-Centric
452 scenario and solely finetuning on Ref-AVS brings high baseline result, adopting our methodologies,
453 **MISA** and **MUSEUM**, significantly improves the result in the Audio-Centric scenario, showcasing
454 the benefits brought by our proposed methods.

455 5.3 ABLATION STUDIES AND QUALITATIVE RESULTS

456 **Augmentation within MUSEUM.** We study the augmentation methods in MUSEUM by using one
457 augmentation at a time. In Table 3, most strategies improve the performance of Audio-Centric
458 individually, and using all the proposed augmentations improves the overall performance.

459 **Studies within MISA.** Domain-specific design is crucial for the Ref-AVS task. Table 4 show that
460 using a specialized encoder MERT (Li et al., 2023b) achieves better results against the general en-
461 coder BEATs (Chen et al., 2023) and Whisper (Radford et al., 2023); Table 6 shows that utilizing
462 AudioCaps (Kim et al., 2019) and MusicQA (Liu et al., 2023b) for alignment helps boost the overall
463 performance against using either one, suggesting the need for large-scale and domain-specific pre-
464 training. In addition, using rejection supervision also shows an improvement (see Table 5), as the
465 performance might be harmed if the segmentation module is trained with a background mask.

486 **Qualitative Results.** Fig. 5 shows two segmentation examples. While EEMC fails to segment correct sounding object with different expressions, **MISA + MUSEUM** segments the correct sounding objects with high quality given Audio-Centric expressions. Note that, due to a lack of audio-signal learning, MISA fails to segment sounding object within specific-scenario, as shown in the second row of Fig. 5(b), suggesting the need for extra augmented dataset for learning from **MUSEUM**.
 487
 488
 489
 490
 491

492 6 CONCLUSIONS 493

494 We propose **MISA**, a Musical-audio Instructed Segmentation Assistant model by integrating and
 495 aligning audio modality into MLLM, which guides the segmentation model to segment object via
 496 learning through audio. To improve the audio awareness capabilities, we introduce **MUSEUM**, a
 497 musical-audio augmentation pipeline to augment audio through separating and sampling sources,
 498 manipulating and mixing to form a new mixture audio, which enriches the audio samples. We also
 499 refine the Ref-AVSBench as **C-Ref-AVSBench** that categorizes expressions into Audio-Centric,
 500 AV-Grounded, and Visual-Centric, to perform modality-specific evaluation. Our method achieves
 501 state-of-the-art performance on both benchmarks, particularly with the Audio-Centric expressions.
 502
 503

504 REFERENCES 505

506 Guoguo Chen, Shuzhou Chai, Guan-Bo Wang, Jiayu Du, Wei-Qiang Zhang, Chao Weng,
 507 Dan Su, Daniel Povey, Jan Trmal, Junbo Zhang, Mingjie Jin, Sanjeev Khudanpur, Shinji
 508 Watanabe, Shuaijiang Zhao, Wei Zou, Xiangang Li, Xuchen Yao, Yongqing Wang, Zhao
 509 You, and Zhiyong Yan. GigaSpeech: An Evolving, Multi-Domain ASR Corpus with
 510 10,000 Hours of Transcribed Audio. In *Interspeech 2021*, pp. 3670–3674. ISCA, August
 511 2021. doi: 10.21437/Interspeech.2021-1965. URL https://www.isca-archive.org/interspeech_2021/chen21o_interspeech.html.
 512 Sanyuan Chen, Yu Wu, Chengyi Wang, Shujie Liu, Daniel Tompkins, Zhuo Chen, Wanxiang Che,
 513 Xiangzhan Yu, and Furu Wei. BEATs: Audio Pre-Training with Acoustic Tokenizers. In *Proceedings of the 40th International Conference on Machine Learning*, pp. 5178–5193. PMLR,
 514 July 2023. URL <https://proceedings.mlr.press/v202/chen23ag.html>. ISSN:
 515 2640-3498.
 516
 517 Zhe Chen, Jiannan Wu, Wenhui Wang, Weijie Su, Guo Chen, Sen Xing, Muyan Zhong, Qinglong
 518 Zhang, Xizhou Zhu, Lewei Lu, Bin Li, Ping Luo, Tong Lu, Yu Qiao, and Jifeng Dai. InternVL:
 519 Scaling up Vision Foundation Models and Aligning for Generic Visual-Linguistic Tasks. In *2024
 520 IEEE/CVF Conference on Computer Vision and Pattern Recognition (CVPR)*, pp. 24185–24198,
 521 2024. URL https://openaccess.thecvf.com/content/CVPR2024/html/Chen_InternVL_Scaling_up_Vision_Foundation_Models_and_Aligning_for_Generic_CVPR_2024_paper.html.
 522
 523
 524 Bowen Cheng, Ishan Misra, Alexander G. Schwing, Alexander Kirillov, and Rohit Girdhar. Masked-
 525 attention Mask Transformer for Universal Image Segmentation. In *2022 IEEE/CVF Conference
 526 on Computer Vision and Pattern Recognition (CVPR)*, pp. 1280–1289, New Orleans, LA, USA,
 527 June 2022. IEEE. ISBN 978-1-6654-6946-3. doi: 10.1109/CVPR52688.2022.00135. URL
 528 <https://ieeexplore.ieee.org/document/9878483/>.
 529
 530 Zesen Cheng, Sicong Leng, Hang Zhang, Yifei Xin, Xin Li, Guanzheng Chen, Yongxin Zhu, Wenqi
 531 Zhang, Ziyang Luo, Deli Zhao, and Lidong Bing. VideoLLaMA 2: Advancing Spatial-Temporal
 532 Modeling and Audio Understanding in Video-LLMs, October 2024. URL <http://arxiv.org/abs/2406.07476>. arXiv:2406.07476 [cs].
 533
 534 Sanjoy Chowdhury, Sayan Nag, Subhrajyoti Dasgupta, Jun Chen, Mohamed Elhoseiny, Ruohan
 535 Gao, and Dinesh Manocha. MEERKAT: Audio-Visual Large Language Model for Ground-
 536 ing in Space and Time. In Aleš Leonardis, Elisa Ricci, Stefan Roth, Olga Russakovsky,
 537 Torsten Sattler, and Gü̈l Varol (eds.), *Computer Vision – ECCV 2024*, volume 15122, pp. 52–
 538 70. Springer Nature Switzerland, Cham, 2025. ISBN 978-3-031-73038-2 978-3-031-73039-
 539 9. doi: 10.1007/978-3-031-73039-9_4. URL https://link.springer.com/10.1007/978-3-031-73039-9_4. Series Title: Lecture Notes in Computer Science.

540 Henghui Ding, Song Tang, Shuting He, Chang Liu, Zuxuan Wu, and Yu-Gang Jiang. Multimodal
 541 Referring Segmentation: A Survey, August 2025. URL <http://arxiv.org/abs/2508.00265> [cs].
 542

543 Henghui Du, Guangyao Li, Chang Zhou, Chunjie Zhang, Alan Zhao, and Di Hu. Crab: A Unified
 544 Audio-Visual Scene Understanding Model with Explicit Cooperation. In *2025 IEEE/CVF
 545 Conference on Computer Vision and Pattern Recognition (CVPR)*, pp. 18804–18814, 2025.
 546 URL https://openaccess.thecvf.com/content/CVPR2025/html/Du_Crab_A_Unified_Audio-Visual_Scene_Understanding_Model_with_Explicit_Cooperation_CVPR_2025_paper.html.
 547

550 Alexandre Défossez, Nicolas Usunier, Léon Bottou, and Francis Bach. Music Source Sepa-
 551 ration in the Waveform Domain, April 2021. URL <http://arxiv.org/abs/1911.13254>.
 552 arXiv:1911.13254 [cs].

553 Shengyi Gao, Zhe Chen, Guo Chen, Wenhui Wang, and Tong Lu. AVSegFormer: Audio-Visual
 554 Segmentation with Transformer. *Proceedings of the AAAI Conference on Artificial Intelligence*,
 555 38(11):12155–12163, March 2024. ISSN 2374-3468. doi: 10.1609/aaai.v38i11.29104. URL
 556 <https://ojs.aaai.org/index.php/AAAI/article/view/29104>.
 557

558 Edward J. Hu, Yelong Shen, Phillip Wallis, Zeyuan Allen-Zhu, Yuanzhi Li, Shean Wang, Lu Wang,
 559 and Weizhu Chen. LoRA: Low-Rank Adaptation of Large Language Models. October 2021.
 560 URL <https://openreview.net/forum?id=nZeVKeeFYf9>.

561 Chang-Bin Jeon, Gordon Wichern, François G. Germain, and Jonathan Le Roux. Why Does Mu-
 562 sic Source Separation Benefit from Cacophony? In *2024 IEEE International Conference on
 563 Acoustics, Speech, and Signal Processing Workshops (ICASSPW)*, pp. 873–877, April 2024.
 564 doi: 10.1109/ICASSPW62465.2024.10669899. URL <https://ieeexplore.ieee.org/document/10669899>.
 565

566 Chris Dongjoo Kim, Byeongchang Kim, Hyunmin Lee, and Gunhee Kim. AudioCaps: Generating
 567 Captions for Audios in The Wild. In Jill Burstein, Christy Doran, and Thamar Solorio (eds.),
 568 *Proceedings of the 2019 Conference of the North American Chapter of the Association for Com-
 569 putational Linguistics: Human Language Technologies, Volume 1 (Long and Short Papers)*, pp.
 570 119–132, Minneapolis, Minnesota, June 2019. Association for Computational Linguistics. doi:
 571 10.18653/v1/N19-1011. URL <https://aclanthology.org/N19-1011/>.
 572

573 Gwantae Kim, David K. Han, and Hanseok Ko. SpecMix : A Mixed Sample Data Augmen-
 574 tation Method for Training with Time-Frequency Domain Features. In *Interspeech 2021*, pp.
 575 546–550. ISCA, August 2021. doi: 10.21437/Interspeech.2021-103. URL https://www.isca-archive.org/interspeech_2021/kim21c_interspeech.html.
 576

577 Alexander Kirillov, Eric Mintun, Nikhila Ravi, Hanzi Mao, Chloe Rolland, Laura Gustafson,
 578 Tete Xiao, Spencer Whitehead, Alexander C. Berg, Wan-Yen Lo, Piotr Dollár, and Ross Gir-
 579 shick. Segment Anything, April 2023. URL <http://arxiv.org/abs/2304.02643> [cs].
 580 arXiv:2304.02643 [cs].

581 Tom Ko, Vijayaditya Peddinti, Daniel Povey, and Sanjeev Khudanpur. Audio augmentation for
 582 speech recognition. pp. 3586–3589, 2015. doi: 10.21437/Interspeech.2015-711. URL https://www.isca-archive.org/interspeech_2015/ko15_interspeech.html#.
 583

584 Xin Lai, Zhuotao Tian, Yukang Chen, Yanwei Li, Yuhui Yuan, Shu Liu, and Jiaya Jia. LISA:
 585 Reasoning Segmentation via Large Language Model. In *2024 IEEE/CVF Conference on
 586 Computer Vision and Pattern Recognition (CVPR)*, pp. 9579–9589, 2024. URL https://openaccess.thecvf.com/content/CVPR2024/html/Lai_LISA_Reasoning_Segmentation_via_Large_Language_Model_CVPR_2024_paper.html.
 587

588

589 Guangyao Li, Yake Wei, Yapeng Tian, Chenliang Xu, Ji-Rong Wen, and Di Hu. Learning to Answer
 590 Questions in Dynamic Audio-Visual Scenarios. In *2022 IEEE/CVF Conference on Computer
 591 Vision and Pattern Recognition (CVPR)*, pp. 19086–19096, New Orleans, LA, USA, June 2022.
 592 IEEE. ISBN 978-1-6654-6946-3. doi: 10.1109/CVPR52688.2022.01852. URL <https://ieeexplore.ieee.org/document/9879157/>.
 593

594 Xiang Li, Jinglu Wang, Xiaohao Xu, Xiao Li, Bhiksha Raj, and Yan Lu. Robust Referring Video
 595 Object Segmentation with Cyclic Structural Consensus. In *2023 IEEE/CVF International Conference on Computer Vision (ICCV)*, pp. 22179–22188, October 2023a. doi: 10.1109/ICCV51070.
 596 2023.02032. URL <https://ieeexplore.ieee.org/document/10378357>. ISSN:
 597 2380-7504.

598 Yizhi Li, Ruibin Yuan, Ge Zhang, Yinghao Ma, Xingran Chen, Hanzhi Yin, Chenghao Xiao,
 599 Chenghua Lin, Anton Ragni, Emmanouil Benetos, Norbert Gyenge, Roger Dannenberg, Ruibo
 600 Liu, Wenhua Chen, Gus Xia, Yemin Shi, Wenhao Huang, Zili Wang, Yike Guo, and Jie Fu. MERT:
 601 Acoustic Music Understanding Model with Large-Scale Self-supervised Training. October 2023b.
 602 URL <https://openreview.net/forum?id=w3YZ9MS1Bu>.

603 Haotian Liu, Chunyuan Li, Qingyang Wu, and Yong Jae Lee. Visual Instruction Tuning, December
 604 2023a. URL <https://arxiv.org/abs/2304.08485>. arXiv:2304.08485 [cs].

605 Shansong Liu, Atin Sakkeer Hussain, Chenshuo Sun, and Ying Shan. Music Understanding LLaMA:
 606 Advancing Text-to-Music Generation with Question Answering and Captioning, August 2023b.
 607 URL <https://arxiv.org/abs/2308.11276>. arXiv:2308.11276 [cs].

608 Yuyuan Liu, Yuanhong Chen, Chong Wang, Junlin Han, Junde Wu, Can Peng, Jingkun Chen,
 609 Yu Tian, and Gustavo Carneiro. AuralSAM2: Enabling SAM2 Hear Through Pyramid Audio-
 610 Visual Feature Prompting, June 2025. URL <https://arxiv.org/abs/2506.01015>.
 611 arXiv:2506.01015 [cs].

612 Ziyang Luo, Nian Liu, Fahad Shahbaz Khan, and Junwei Han. AURORA: Augmented Under-
 613 standing via Structured Reasoning and Reinforcement Learning for Reference Audio-Visual Seg-
 614 mentation, August 2025. URL <https://arxiv.org/abs/2508.02149>. arXiv:2508.02149 [cs]
 615 version: 1.

616 Brian McFee, Matt McVicar, Daniel Faroni, Iran Roman, Matan Gover, Stefan Balke, Scott Sey-
 617 farth, Ayoub Malek, Colin Raffel, Vincent Lostanlen, Benjamin van Niekerk, Dana Lee, Frank
 618 Cwitkowitz, Frank Zalkow, Oriol Nieto, Dan Ellis, Jack Mason, Kyungyun Lee, Bea Steers,
 619 Emily Halvachs, Carl Thomé, Fabian Robert-Stöter, Rachel Bittner, Ziyao Wei, Adam Weiss, Eric
 620 Battenberg, Keunwoo Choi, Ryuichi Yamamoto, C. J. Carr, Alex Metsai, Stefan Sullivan, Pius
 621 Friesch, Asmitha Krishnakumar, Shunsuke Hidaka, Steve Kowalik, Fabian Keller, Dan Mazur,
 622 Alexandre Chabot-Leclerc, Curtis Hawthorne, Chandrashekhar Ramaprasad, Myungchul Keum,
 623 Juanita Gomez, Will Monroe, Viktor Andreevitch Morozov, Kian Eliasi, nullmightybofo, Paul
 624 Biberstein, N. Dorukhan Sergin, Romain Hennequin, Rimvydas Naktinis, beantowel, Taewoon
 625 Kim, Jon Petter Åsen, Joon Lim, Alex Malins, Darío Hereñú, Stef van der Struijk, Lorenz Nickel,
 626 Jackie Wu, Zhen Wang, Tim Gates, Matt Vollrath, Andy Sarroff, Xiao-Ming, Alastair Porter, Seth
 627 Kranzler, Voodoohop, Mattia Di Gangi, Helmi Jinoz, Connor Guerrero, Abduttayyeb Mazhar,
 628 toddrme2178, Zvi Baratz, Anton Kostin, Xinlu Zhuang, Cash TingHin Lo, Pavel Campr, Eric
 629 Se-
 630 meniuc, Monsij Biswal, Shayenne Moura, Paul Brossier, Hojin Lee, Waldir Pimenta, Jon Petter
 631 Åsen, Shin Hyun, Iliya S, Eugene Rabinovich, Geo Lei, Jize Guo, Phillip S. M. Skelton, Matt
 632 Pitkin, Anmol Mishra, Slava Chaunin, BenedictSt, Scott VanRavenswaay, and David Südholz.
 633 librosa/librosa: 0.11.0, March 2025. URL <https://zenodo.org/records/15006942>.

634 Linghui Meng, Jin Xu, Xu Tan, Jindong Wang, Tao Qin, and Bo Xu. MixSpeech: Data Augmen-
 635 tation for Low-Resource Automatic Speech Recognition. In *ICASSP 2021 - 2021 IEEE Interna-
 636 tional Conference on Acoustics, Speech and Signal Processing (ICASSP)*, pp. 7008–7012, June
 637 2021. doi: 10.1109/ICASSP39728.2021.9414483. URL <https://ieeexplore.ieee.org/document/9414483>. ISSN: 2379-190X.

638 Daniel S. Park, William Chan, Yu Zhang, Chung-Cheng Chiu, Barret Zoph, Ekin D. Cubuk, and
 639 Quoc V. Le. SpecAugment: A Simple Data Augmentation Method for Automatic Speech
 640 Recognition. In *Interspeech 2019*, pp. 2613–2617. ISCA, September 2019. doi: 10.21437/
 641 Interspeech.2019-2680. URL https://www.isca-archive.org/interspeech_2019/park19e_interspeech.html.

642 Laure Prétet, Romain Hennequin, Jimena Royo-Letelier, and Andrea Vaglio. Singing Voice Sep-
 643 aration: A Study on Training Data. In *ICASSP 2019 - 2019 IEEE International Conference on
 644 Acoustics, Speech and Signal Processing (ICASSP)*, pp. 506–510, Brighton, United Kingdom,

648 May 2019. IEEE. doi: 10.1109/ICASSP.2019.8683555. URL <https://telecom-paris.hal.science/hal-02372076>.

649

650

651 Qwen, An Yang, Baosong Yang, Beichen Zhang, Binyuan Hui, Bo Zheng, Bowen Yu, Chengyuan

652 Li, Dayiheng Liu, Fei Huang, Haoran Wei, Huan Lin, Jian Yang, Jianhong Tu, Jianwei Zhang,

653 Jianxin Yang, Jiaxi Yang, Jingren Zhou, Junyang Lin, Kai Dang, Keming Lu, Keqin Bao, Kexin

654 Yang, Le Yu, Mei Li, Mingfeng Xue, Pei Zhang, Qin Zhu, Rui Men, Runji Lin, Tianhao Li,

655 Tianyi Tang, Tingyu Xia, Xingzhang Ren, Xuancheng Ren, Yang Fan, Yang Su, Yichang Zhang,

656 Yu Wan, Yuqiong Liu, Zeyu Cui, Zhenru Zhang, and Zihan Qiu. Qwen2.5 Technical Report,

657 January 2025. URL <http://arxiv.org/abs/2412.15115>. arXiv:2412.15115 [cs].

658

659 Alec Radford, Jong Wook Kim, Tao Xu, Greg Brockman, Christine McLeavey, and Ilya Sutskever.

660 Robust speech recognition via large-scale weak supervision. In *Proceedings of the 40th International Conference on Machine Learning*, volume 202 of *ICML’23*, pp. 28492–28518, Honolulu, Hawaii, USA, 2023. JMLR.org.

661

662 Abduljalil Radman and Jorma Laaksonen. TSAM: Temporal SAM Augmented with Multi-

663 modal Prompts for Referring Audio-Visual Segmentation. In *2025 IEEE/CVF Conference on Computer Vision and Pattern Recognition (CVPR)*, pp. 23947–23956, 2025. URL https://openaccess.thecvf.com/content/CVPR2025/html/Radman_TSAM_Temporal_SAM_Augmented_with_Multimodal_Prompts_for_Referring_Audio-Visual_CVPR_2025_paper.html.

664

665

666

667

668 Nikhila Ravi, Valentin Gabeur, Yuan-Ting Hu, Ronghang Hu, Chaitanya Ryali, Tengyu Ma, Haitham

669 Khedr, Roman Rädle, Chloe Rolland, Laura Gustafson, Eric Mintun, Junting Pan, Kalyan Va-

670 sudev Alwala, Nicolas Carion, Chao-Yuan Wu, Ross Girshick, Piotr Dollár, and Christoph Fe-

671 ichtenhofer. SAM 2: Segment Anything in Images and Videos, October 2024. URL <http://arxiv.org/abs/2408.00714>. arXiv:2408.00714 [cs].

672

673

674 Simon Rouard, Francisco Massa, and Alexandre Défossez. Hybrid Transformers for Mu-

675 sic Source Separation, November 2022. URL <http://arxiv.org/abs/2211.08553>.

676 arXiv:2211.08553 [eess].

677

678 Stefan Uhlich, Marcello Porcu, Franck Giron, Michael Enenkl, Thomas Kemp, Naoya Takahashi,

679 and Yuki Mitsufuji. Improving music source separation based on deep neural networks through

680 data augmentation and network blending. In *2017 IEEE International Conference on Acoustics,*

681 *Speech and Signal Processing (ICASSP)*, pp. 261–265, March 2017. doi: 10.1109/ICASSP.2017.

682 7952158. URL <https://ieeexplore.ieee.org/document/7952158>. ISSN: 2379-

683 190X.

684

685 Yaoting Wang, Weisong Liu, Guangyao Li, Jian Ding, Di Hu, and Xi Li. Prompting segmentation

686 with sound is generalizable audio-visual source localizer. In *Proceedings of the Thirty-Eighth*

687 *AAAI Conference on Artificial Intelligence and Thirty-Sixth Conference on Innovative Applica-*

688 *tions of Artificial Intelligence and Fourteenth Symposium on Educational Advances in Artificial*

689 *Intelligence*, volume 38 of *AAAI’24/IAAI’24/EAAI’24*, pp. 5669–5677. AAAI Press, 2024a. ISBN

690 978-1-57735-887-9. doi: 10.1609/aaai.v38i6.28378. URL <https://doi.org/10.1609/aaai.v38i6.28378>.

691

692 Yaoting Wang, Peiwen Sun, Dongzhan Zhou, Guangyao Li, Honggang Zhang, and Di Hu. Ref-

693 avs: Refer and segment objects in audio-visual scenes. *IEEE European Conference on Computer*

694 *Vision (ECCV)*, 2024b.

695

696 Yuji Wang, Haoran Xu, Yong Liu, Jiaze Li, and Yansong Tang. SAM2-LOVE: Seg-

697 ment Anything Model 2 in Language-aided Audio-Visual Scenes. In *2025 IEEE/CVF*

698 *Conference on Computer Vision and Pattern Recognition (CVPR)*, pp. 28932–28941,

699 2025a. URL https://openaccess.thecvf.com/content/CVPR2025/html/Wang_SAM2-LOVE_SegmentAnything_Model_2_in_Language-aided_Audio-Visual_Scenes_CVPR_2025_paper.html.

700

701 Zaitian Wang, Pengfei Wang, Kunpeng Liu, Pengyang Wang, Yanjie Fu, Chang-Tien Lu, Charu C.

702 Aggarwal, Jian Pei, and Yuanchun Zhou. A Comprehensive Survey on Data Augmentation, May

703 2025b. URL <http://arxiv.org/abs/2405.09591>. arXiv:2405.09591 [cs].

702 Jason Wei, Xuezhi Wang, Dale Schuurmans, Maarten Bosma, brian ichter, Fei Xia, Ed Chi, Quoc V
 703 Le, and Denny Zhou. Chain-of-Thought Prompting Elicits Reasoning in Large Language Mod-
 704 els. In S. Koyejo, S. Mohamed, A. Agarwal, D. Belgrave, K. Cho, and A. Oh (eds.), *Advances in*
 705 *Neural Information Processing Systems*, volume 35, pp. 24824–24837. Curran Associates, Inc.,
 706 2022. URL https://proceedings.neurips.cc/paper_files/paper/2022/file/9d5609613524ecf4f15af0f7b31abca4-Paper-Conference.pdf.

707
 708 Jiannan Wu, Yi Jiang, Peize Sun, Zehuan Yuan, and Ping Luo. Language As Queries for Referring
 709 Video Object Segmentation. In *2022 IEEE/CVF Conference on Computer Vision and Pattern*
 710 *Recognition (CVPR)*, pp. 4974–4984, 2022. URL https://openaccess.thecvf.com/content/CVPR2022/html/Wu_Language_As_Queries_for_Referring_Video_Object_Segmentation_CVPR_2022_paper.html.

711
 712 Jin Xu, Zhifang Guo, Jinzheng He, Hangrui Hu, Ting He, Shuai Bai, Keqin Chen, Jialin Wang, Yang
 713 Fan, Kai Dang, Bin Zhang, Xiong Wang, Yunfei Chu, and Junyang Lin. Qwen2.5-Omni Technical
 714 Report, March 2025. URL <http://arxiv.org/abs/2503.20215>. arXiv:2503.20215
 715 [cs].

716
 717 Cilin Yan, Haochen Wang, Shilin Yan, Xiaolong Jiang, Yao Hu, Guoliang Kang, Weidi Xie, and
 718 Efstratios Gavves. VISA: Reasoning Video Object Segmentation via Large Language Models. In
 719 *Computer Vision – ECCV 2024: 18th European Conference, Milan, Italy, September 29–October*
 720 *4, 2024, Proceedings, Part XV*, pp. 98–115, Berlin, Heidelberg, 2024. Springer-Verlag. ISBN 978-
 721 3-031-72632-3. doi: 10.1007/978-3-031-72633-0_6. URL https://doi.org/10.1007/978-3-031-72633-0_6.

722
 723 Kaining Ying, Henghui Ding, Guangquan Jie, and Yu-Gang Jiang. Towards Omnimodal Expressions
 724 and Reasoning in Referring Audio-Visual Segmentation, July 2025. URL <http://arxiv.org/abs/2507.22886> [cs] version: 2.

725
 726 Wenhao You, Xingjian Diao, Chunhui Zhang, Keyi Kong, Weiyi Wu, Zhongyu Ouyang, Chiyu Ma,
 727 Tingxuan Wu, Noah Wei, Zong Ke, Ming Cheng, Soroush Vosoughi, and Jiang Gui. Music’s
 728 Multimodal Complexity in AVQA: Why We Need More than General Multimodal LLMs, May
 729 2025. URL <http://arxiv.org/abs/2505.20638>. arXiv:2505.20638 [cs].

730
 731 Haobo Yuan, Xiangtai Li, Tao Zhang, Zilong Huang, Shilin Xu, Shunping Ji, Yunhai Tong, Lu Qi, Ji-
 732 ashi Feng, and Ming-Hsuan Yang. Sa2VA: Marrying SAM2 with LLaVA for Dense Grounded Un-
 733 derstanding of Images and Videos, February 2025. URL <http://arxiv.org/abs/2501.04001>. arXiv:2501.04001 [cs].

734
 735 Hang Zhao, Chuang Gan, Wei-Chiu Ma, and Antonio Torralba. The Sound of Motions. pp.
 736 1735–1744, 2019. URL https://openaccess.thecvf.com/content_ICCV_2019_html/Zhao_The_Sound_of_Motions_ICCV_2019_paper.html.

737
 738 Hao Zhong, Muzhi Zhu, Zongze Du, Zheng Huang, Canyu Zhao, Mingyu Liu, Wen Wang, Hao
 739 Chen, and Chunhua Shen. Omni-R1: Reinforcement Learning for Omnimodal Reasoning via
 740 Two-System Collaboration, May 2025. URL <http://arxiv.org/abs/2505.20256>.
 741 arXiv:2505.20256 [cs].

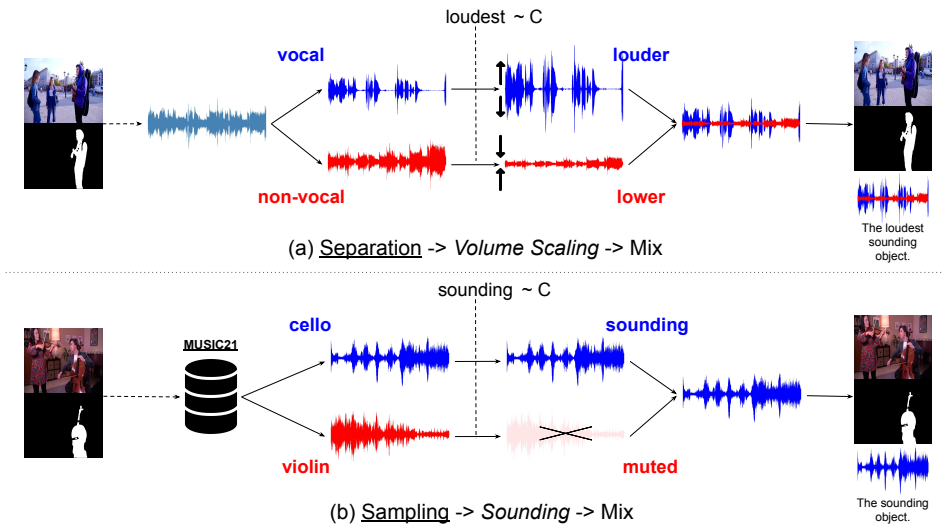
742
 743 Jinxing Zhou, Jianyuan Wang, Jiayi Zhang, Weixuan Sun, Jing Zhang, Stan Birchfield, Dan Guo,
 744 Lingpeng Kong, Meng Wang, and Yiran Zhong. Audio–Visual Segmentation. In Shai Avidan,
 745 Gabriel Brostow, Moustapha Cissé, Giovanni Maria Farinella, and Tal Hassner (eds.), *Computer*
 746 *Vision – ECCV 2022*, pp. 386–403, Cham, 2022. Springer Nature Switzerland. ISBN 978-3-031-
 747 19836-6. doi: 10.1007/978-3-031-19836-6_22.

748
 749 Jinxing Zhou, Xuyang Shen, Jianyuan Wang, Jiayi Zhang, Weixuan Sun, Jing Zhang, Stan
 750 Birchfield, Dan Guo, Lingpeng Kong, Meng Wang, and Yiran Zhong. Audio-Visual Seg-
 751 mentation with Semantics, January 2023. URL <http://arxiv.org/abs/2301.13190>.
 752 arXiv:2301.13190 [cs].

753
 754 Jinxing Zhou, Yanghao Zhou, Mingfei Han, Tong Wang, Xiaojun Chang, Hisham Cholakkal, and
 755 Rao Muhammad Anwer. Think Before You Segment: An Object-aware Reasoning Agent for Re-
 ferring Audio-Visual Segmentation, August 2025. URL <http://arxiv.org/abs/2508.04418>. arXiv:2508.04418 [cs].

756
757 **Table 7: Function of Augmentation Eq. 5.** We organize keywords into multiple types, using the
758 same augmentation method. Target Signal $s^{(tgt)}$, Reference Signal $s^{(ref)}$, and c are the inputs.
759 Given c , each input uses its parameters with the corresponding method. We specify the parameters
760 to produce 10-second audio signal as follows: $\alpha_{min}^+ = 1.25$; $\alpha_{max}^+ = 1.5$; $\alpha_{min}^- = 0.3$; $\alpha_{max}^- =$
761 0.5 ; $\gamma_{min}^+ = 1.25$; $\gamma_{max}^+ = 1.5$; $\gamma_{min}^- = 0.3$; $\gamma_{max}^- = 0.5$; $\Delta t \sim U(1, 5) \cdot \text{sampling rate}$.

Type	Keywords (c)	Method	Target Signal ($s^{(tgt)}$)	Reference Signal ($s^{(ref)}$)
Volume	Loudest	$\tilde{s}(t) = \alpha \cdot s(t)$.	$\alpha \sim U(\alpha_{min}^+, \alpha_{max}^+)$	$\alpha \sim U(\alpha_{min}^-, \alpha_{max}^-)$
Volume	Lowest	$\tilde{s}(t) = \alpha \cdot s(t)$.	$\alpha \sim U(\alpha_{min}^-, \alpha_{max}^-)$	$\alpha \sim U(\alpha_{min}^+, \alpha_{max}^+)$
Rhythm	Fastest	$\tilde{s}(t) = s(\gamma \cdot t)$.	$\gamma \sim U(\gamma_{min}^+, \gamma_{max}^+)$	$\gamma \sim U(\gamma_{min}^-, \gamma_{max}^-)$
Rhythm	Slowest	$\tilde{s}(t) = s(\gamma \cdot t)$.	$\gamma \sim U(\gamma_{min}^-, \gamma_{max}^-)$	$\gamma \sim U(\gamma_{min}^+, \gamma_{max}^+)$
Temporal	First	$\tilde{s}(t) = \mathbf{1}[t \notin \mathcal{T}] \cdot s(t)$.	$\mathcal{T} = \emptyset$	$\mathcal{T} = [0, \Delta t]$
Temporal	Last	$\tilde{s}(t) = \mathbf{1}[t \notin \mathcal{T}] \cdot s(t)$.	$\mathcal{T} = \emptyset$	$\mathcal{T} = [T - \Delta t, T]$
Temporal	Longest	$\tilde{s}(t) = \mathbf{1}[t \notin \mathcal{T}] \cdot s(t)$.	$\mathcal{T} = \emptyset$	$\mathcal{T} = [t_0, t_0 + \Delta t]$
Temporal	Shortest	$\tilde{s}(t) = \mathbf{1}[t \notin \mathcal{T}] \cdot s(t)$.	$\mathcal{T} = [t_0, t_0 + \Delta t]$	$\mathcal{T} = \emptyset$
Sounding	Sounding	$\tilde{s}(t) = \mathbf{1}[t \notin \mathcal{T}] \cdot s(t)$.	$\mathcal{T} = \emptyset$	$\mathcal{T} = [0, T]$
Muted	Muted	$\tilde{s}(t) = \mathbf{1}[t \notin \mathcal{T}] \cdot s(t)$.	$\mathcal{T} = [0, T]$	$\mathcal{T} = \emptyset$



793 **Figure 6: Examples of the MUSEUM workflow.** (a) Given a video of a man and a guitar, mask
794 refers to the man, it separates the vocal and non-vocal sound to individual signal from original
795 source, assign **vocal** as target and **non-vocal** as reference given mask’s category; given sampled
796 keyword “loudest”, it performs volume scaling by scaling up the amplitude of the target signal,
797 scaling down the amplitude of the reference signal. (b) Given a video of a violin and a cello, mask
798 refers to the cello; it samples the violin and cello sources from MUSIC21 (Zhao et al., 2019), assigns
799 **cello** as target and **violin** as reference; given sampled keyword “sounding”, retain the target signal,
800 mask the reference signal. Both examples operate by mixing two augmented signals to a mixture
801 signal, producing new visual-mask-audio-text samples with sampled expressions.

A APPENDIX

A.1 DETAILS OF MUSEUM.

807 We provide the details of MUSEUM, particularly the composition of the augmentation stage F_{aug}
808 shown in Table 7; examples of the sample augmentation workflow in Fig. 6; the MUSEUM Aug-
809 mentation Algorithm 1; and examples of the expressions template E , which we used for MUSEUM
810 augmented signal expression construction, shown in Table 8

810
 811 **Algorithm 1:** MUSEUM Augmentation Pipeline.
 812 **Input:** Input dataset D , num. of samples \tilde{N} , expressions template E , keywords C
 813 **Output:** Augmented dataset \tilde{D}
 814 sample $D_{sep}, D_{samp} \sim D$;
 815 $\tilde{D} \leftarrow \emptyset, j \leftarrow 0$;
 816 **while** $j < \tilde{N}$ **do**
 817 sample keyword $c \sim C$;
 818 sample $d = \{d^{(v)}, d^{(m)}, d^{(s)}\} \sim D$;
 819 assign $c^{(tgt)}, c^{(ref)}$ given $d^{(m)}$;
 820 **if** $d \in D_{sep}$ **then**
 821 | assign $s^{(tgt)}, s^{(ref)}$ according to Eq. 2 and Eq. 3;
 822 **end**
 823 **else if** $d \in D_{samp}$ **then**
 824 | assign $s^{(tgt)}, s^{(ref)}$ according to Eq. 4;
 825 **end**
 826 **else**
 827 | skip current step;
 828 **end**
 829 assign $\tilde{s}^{(tgt)}, \tilde{s}^{(ref)}$ according to Eq. 5 and Table 7;
 830 $\tilde{s} \leftarrow \tilde{s}^{tgt} + \tilde{s}^{ref}$;
 831 sample expression $e \sim E|c$;
 832 $\tilde{d} \leftarrow \{d^{(v)}, d^{(m)}, \tilde{s}, e\}$;
 833 $\tilde{D} \leftarrow \tilde{D} \cup \{\tilde{d}\}$;
 834 $j \leftarrow j + 1$;
 835 **end**
 836
 837

838 The main objective is to synthesize an augmented dataset \tilde{D} given D for model training. Using this
 839 methodology, we can augment each sample d drawn from D with a different combination of acous-
 840 tic properties (e.g., louder violin sound and lower cello sound), simulating various mixture sources.
 841 This is achieved by identifying the target $c^{(tgt)}$ and reference $c^{(ref)}$, which can be processed from orig-
 842 inal dataset ($D_{sep}, D_{samp} \sim D$, D_{sep} corresponds to vocal/non-vocal subset while D_{samp} corre-
 843 sponds to multiple music instruments subset), extracting the target and reference signal $s^{(tgt)}, s^{(ref)}$,
 844 augmenting each signal to $\tilde{s}^{(tgt)}, \tilde{s}^{(ref)}$, and mixing both to \tilde{s} (demonstrated in Algorithm 1). To
 845 align with the sampled keyword $c \sim C$ (denotes the predefined keywords set), we carefully manip-
 846 ulate the audio signals for target $s^{(tgt)}$ and reference $s^{(ref)}$ with a different predefined parameter,
 847 shown in Table 7. By considering various scenarios, we obtain sources from either vocal/non-vocal
 848 D_{sep} or multiple instruments D_{samp} audio-visual scenes, which we can identify by the metadata
 849 from the dataset, and use as a condition for stage execution within the musical source stage. Fig. 6
 850 showed two examples of an augmentation workflow, one utilized a separation path and another
 851 utilized a sampling path, demonstrating the workflow of signal extraction, augmentation given a
 852 keyword, and mixing to form an augmented sample.

853
 854 A.2 DETAILS OF C-REF-AVSBENCH.
 855
 856 Table 9 shows both Ref-AVSBench’s and C-Ref-AVSBench’s statistics. Approximately 60% of
 857 videos in Ref-AVSBench are part of the Ref-AVS training set. Removing these helps us to evaluate
 858 performance in fair conditions, compared to the visual-text baseline. Fig. 7 shows an example. The
 859 video exists in both training and testing sets, with different timestamps. They share similar visual
 860 scenes, exhibit identical expressions and answers across the training and testing sets, making them
 861 overoptimistic in evaluating certain cases.

862 Table 10 lists examples of each label. While the expressions do not contain any acoustic keyword
 863 like “sound” or “sing”, the expressions are labeled as Visual-Centric; While the expressions exist
 864 both acoustic keywords and the semantic/explicit (e.g., “boy”, “piano”, “standing”), spatial (e.g.,

864

865

Table 8: **Expressions Template E.** We listed 2 examples per keyword.

Keyword	Expressions
Loudest	The object making the loudest sound. The object with the highest volume.
Lowest	The object making the lowest sound. The object with the lowest volume.
Fastest	The object making the fastest rhythm. The object with the fastest tempo.
Slowest	The object making the slowest rhythm. The object with the slowest tempo.
First	The first object making the sound. The first object emitting the sound.
Last	The last object making the sound. The last object emitting the sound.
Longest	The object with the longest sound duration. The object making the longest sound duration.
Shortest	The object with the shortest sound duration. The object making the shortest sound duration.
Sounding	The object making the sound. The sounding object.
Muted	The instrument is muted. The instrument didn't make any sound.

890

891

892

Table 9: **Statistics of C-Ref-AVSBench.**

Dataset	Uniq. Video	Overall	Audio-Centric	AV-Grounded	Visual-Centric	Volume	Temporal	Rhythm
Ref-AVSBench Seen	273	2288	630	1115	543	90	113	64
C-Ref-AVSBench	115	918	308	432	178	31	62	20

893

894

895

896

897

898

899

900

901

902

903

904

905

906

907

“left of the”) queries, the expressions are labeled as AV-Grounded; Otherwise, the expressions are labeled as Audio-Centric as these expressions containing only acoustic keywords. As the example of Audio-Centric showed in the Table 10, it can further splitted samples to specific acoustic expression type, denoted as Volume (e.g., “loudest sound”), Rhythm (e.g., “faster rhythm”), and Temporal (e.g., “shortest sound duration”, “making sound at all times”) for specific evaluation. These expressions also guide us in constructing the MUSEUM expressions template as in Table 8 for consistency with Ref-AVS.

A.3 MORE ABLATION STUDIES.

908

909

910

911

912

913

914

915

916

917

Ablation study of samples construction. We compare MUSEUM with heuristic methods. Since our method MUSEUM is a type of resample and dataset extension method, we experiment with two heuristic method: oversample the Audio-Centric as its limitation of sample scale in the original training set; and joint training with an external dataset, MUSIC-AVQA (Li et al., 2022), which included cases as similar as our Audio-Centric type, with a different objective (pure language generation without segmentation). As shown in Table 11, these two methods suffer a performance drop, particularly due to overfitting in the over-sampling cases, and domain gap from other datasets. Our method augments the existing dataset to maintain domain difference and increase variation instead of training with multiple copies. In addition, we also study the sample scale setup of MUSEUM. Controlling the scale approximately the same as the original training set could achieve a better result, as shown in Table 12.



Figure 7: **Example of video exists in both training and testing set.** The video ID is **Pe1LuVFTczE**.

Table 10: **Examples of each expressions type.** We listed 5 examples per type.

Type	Expressions
Audio-Centric	The object making the loudest sound. The object making a sound with a faster rhythm. The object making the shortest sound duration. The object that keeps making sound at all times. The source of the sound.
AV-Grounded	The boy playing ukulele and singing. The object making a sound by being played by the woman. The object making a sound by being played by the man keeping standing. The object making louder sound than the piano. The violin on the left of the sounding piano.
Visual-Centric	The object being held by the woman. The object being played by the individual on the right. The yellow guitar. The boy behind the guitar The object play an instrument standing in the middle.

Ablation study of hyperparameter. We show the hyperparameter studies in the Table 13. The improvement within the model and the parameters achieved by switching SAM (Kirillov et al., 2023) to SAM 2 (Ravi et al., 2024) suggests the stronger segmentation capabilities brought by SAM 2, even without pretrained knowledge from the integration of MLLM; Using a larger LoRA (Hu et al., 2021) rank also helps improve overall performance. While these tweaks help achieve a better foundation performance for all scenarios, using our proposed method, particularly integrating with the domain-specific audio encoder MERT (Li et al., 2023b) and our augmentation dataset MUSEUM, improves the performance within the Audio-Centric scenario. In addition, using MERT as an audio encoder and/or an augmented dataset MUSEUM could also benefit from a relatively weaker setup (the first three rows), with the considerable improvement through the Audio-Centric group, suggesting the significant effectiveness of our methodologies.

A.4 MORE QUALITATIVE RESULTS.

Fig. 8 shows an audio-visual scene with all types of expressions for the two audible objects, with each segmentation methodology's results and metrics. Our method, MISA + MUSEUM, could handle well within all scenarios, compared to EEMC and visual-text SOTA: Sa2VA-1B (finetuned), particularly for the Audio-Centric expressions. Throughout our definition of expressions, we could

972

973

Table 11: **Ablation study of data samples.** Results report with \mathcal{J} & \mathcal{F} .

974

Method	Audio-Centric	Overall	V.	T.	R.
-	81.7	83.2	73.7	79.1	68.8
w/. Oversample	79.8	82.2	73.5	78.2	64.7
w/. MUSIC-AVQA	77.0	80.7	60.7	71.5	62.1
MUSEUM (Ours)	86.4	84.8	83.9	83.9	90.2

975

976

977

978

979

980

981

Table 13: **Ablation study of hyperparameter.** Blue row is our best model.

982

983

Audio Enc.	LoRA	Seg.	Arch.	Pretrained Weights	MUSEUM	Ref-AVS Benchmark			C-Ref-AVS Benchmark					
						\mathcal{J}	\mathcal{F}	$\mathcal{J} \& \mathcal{F}$	\mathcal{J}	\mathcal{F}	$\mathcal{J} \& \mathcal{F}$	Overall	Audio-Centric	
MERT	8	SAM	InternVL2.5-VL-1B & SAM		✓	69.8	81.5	75.7	70.1	82.9	76.5	70.1	83.7	76.9
MERT	8	SAM	InternVL2.5-VL-1B & SAM			66.4	78.9	72.6	67.5	80.3	73.9	67.2	80.4	73.8
BEATs	8	SAM	InternVL2.5-VL-1B & SAM		✓	63.8	77.6	70.7	65.7	79.4	72.6	68.1	82.9	75.5
BEATs	8	SAM	InternVL2.5-VL-1B & SAM			47.9	64.0	55.9	53.0	68.0	60.5	57.9	73.6	65.8
BEATs	8	SAM 2	InternVL2.5-VL-1B & SAM 2			71.2	82.4	76.8	70.8	82.9	76.8	67.3	82.1	74.7
BEATs	8	SAM 2	Sa2VA-1B			70.3	81.9	76.1	71.0	83.0	77.0	68.3	81.2	74.7
BEATs	128	SAM 2	Sa2VA-1B			75.6	86.0	80.8	76.7	87.6	82.2	73.2	85.8	79.5
MERT	128	SAM 2	Sa2VA-1B		✓	76.4	86.5	81.4	78.1	88.3	83.2	76.2	87.2	81.7
MERT	128	SAM 2	Sa2VA-1B			77.0	87.0	82.0	79.9	89.7	84.8	81.6	91.2	86.4

991

992

993

994

995

996

997

998

999

1000

1001

1002

1003

1004

1005

1006

1007

1008

1009

1010

1011

1012

1013

1014

1015

1016

1017

1018

1019

1020

1021

1022

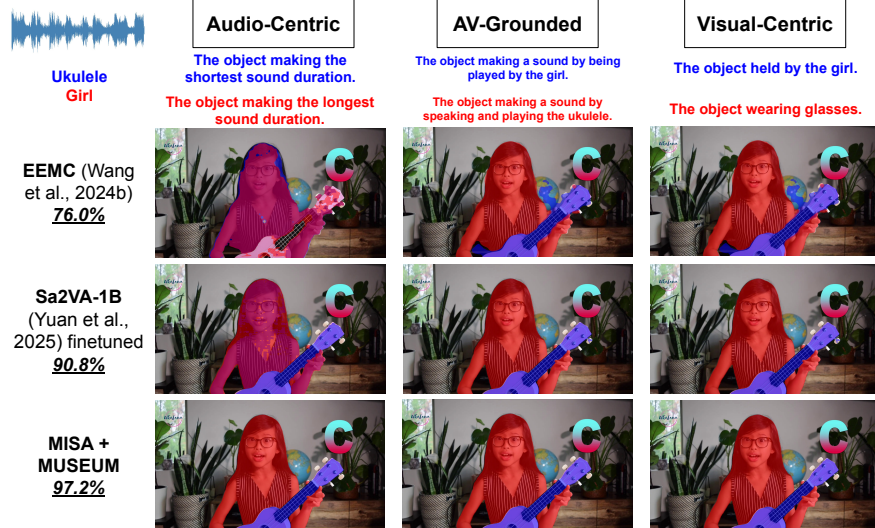
1023

1024

1025

Table 12: **Ablation study of samples size.** Results report with \mathcal{J} & \mathcal{F} .

Ref-AVS : MUSEUM	Audio-Centric	Overall	V.	T.	R.
1 : 0.1	82.6	82.9	79.0	82.5	66.8
1 : 0.5	83.0	83.4	74.8	83.0	83.9
1 : 1 (Ours)	86.4	84.8	83.9	83.9	90.2

Figure 8: **Qualitative results across expressions group.** We compare our methods with SOTAs, and include the average \mathcal{J} & \mathcal{F} of the samples for each model.

easily identify the weakness within each scenario. At the same time, it also suggests the need for precise evaluation and a complete benchmark for some instances.